

Finite element analysis of equal channel angular pressing by using a multi-pass die

R. COMANECI^{a,*}, L. G. BUJOREANU^a, C. BACIU, A. M. PREDESCU^b, D. SAVASTRU^c

^aTechnical University “Gheorghe Asachi” Iasi, D. Mangeron 61A, Iasi, Romania

^b“Politehnica” University of Bucharest, Splaiul Independentei 313, Bucharest, Romania

^cInstitute of Research and Development in Optoelectronics, 409 Atomistilor Street, Magurele, Romania

Equal channel angular pressing (ECAP) is a well-established method for grain refinement in metallic materials by large shear. ECAP is a discontinuous process, so a new sample pushes out the previous sample. As a result, the head and the tail of the sample become strongly distorted, and they must be removed for the next pass, leading to a smaller work piece, pass by pass. To avoid the decreasing in length of the work piece, a multi-pass ECAP without removing the work piece from the die was investigated. Experimental ECAP using a special die having 5 orthogonal channels and dedicated hydraulic pistons was performed successfully. A complete processing cycle consisting of 4 passes via route B_C balanced the wellknown nonuniformity of the strain during ECAP. To get the overall behavior of the material and the accumulated strain distribution history, a 3D finite element analysis was performed. Experimental tests and hardness measurements using tracking point method were conducted in order to validate the simulation, thus completing the study. The results create opportunities in developing integrated systems designed to perform different ECAP routes for any imposed number of passes.

(Received June 6, 2015; accepted September 9, 2015)

Keywords: Equal channel angular pressing, Finite element analysis, Strain, Aluminum

1. Introduction

In last decades, the importance of severe plastic deformation (SPD) and particularly of equal channel angular pressing (ECAP) has been considered thanks to spectacular mechanical properties reached in obtained ultrafine-grained (UFG) materials [1-4].

ECAP is a discontinuous process able to impart high strain in materials through simple shear. The sample is extruded through a die containing two identical cross-sectional channels (Fig. 1). In the extrusion process, the billet crosses the area corresponding to the bisecting plane of the two channels being subjected to simple shearing [5]. The microstructure of the ECAPed material is strongly influenced by the die geometry and extrusion settings that govern the material behavior during shear deformation.

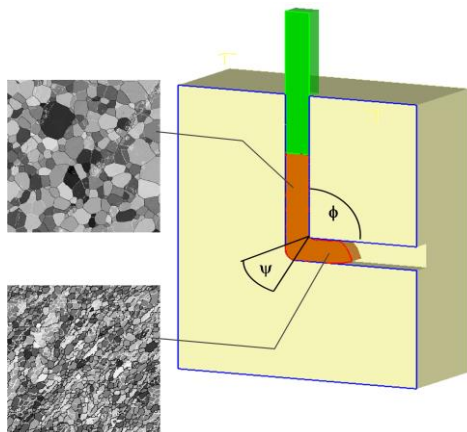


Fig. 1. Schematic illustration of ECAP

Taking into account the die geometry defined by the channel angle ϕ (typically in range of 90-150°) and angle ψ corresponding to the outer fillet radius of the two die channels, Iwahashi et al. [6] calculated the theoretical effective strain $\bar{\epsilon}$ as follows:

$$\bar{\epsilon} = \frac{1}{\sqrt{3}} \left[2 \operatorname{ctg} \left(\frac{\phi}{2} + \frac{\psi}{2} \right) + \psi \cos \operatorname{ec} \left(\frac{\phi}{2} + \frac{\psi}{2} \right) \right] \quad (1)$$

Note that Eq. (1) is a geometrical approach that doesn't include the effect of friction, strain hardening, heterogeneous strain distribution and deformation gradient. It gives a quantitative estimation of strain/pass. For $\phi = 90^\circ$ and $\psi = 0^\circ$ the theoretical strain is 1.15.

The most important technological aspect of the process is that the shape and dimensions of the billet cross-section do not change during extrusion, so that there is no geometric restriction on the strain that can be theoretically reached. The necessary level of the accumulated strain can be achieved by re-inserting billet and resuming extrusion. The billet removal can be done in two ways. Either a new sample is inserted in the vertical channel, forcing the previous sample to move through the horizontal channel or the billet is simply pushed out through the horizontal channel by an additional punch that acts as a pusher. In the first case, the die is a common one but the bent head and the distorted tail have to be removed with inherent loss of volume that can reach even 40% of the starting volume. In the second case, the die is more complicated but no additional operation is required.

To become more effective, the grain refinement can be increased by rotating billet around its longitudinal axis. Four processing routes were tested: route A without rotation, route B_A and B_C with alternating $\pm 90^\circ$ and same sense 90° rotations respectively, and route C with 180° rotations (Fig. 2).

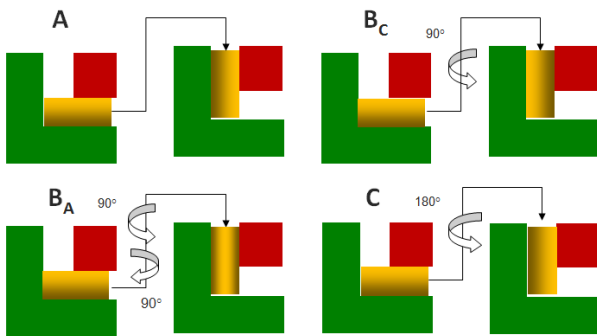


Fig. 2. The processing routes in traditional ECAP

The effects of processing routes on grain refinement are different. According to Zhu and Lowe [7] in multi-pass ECAP_{90°} ($\phi = 90^\circ$) the best grain refinement for fcc Al and its alloys corresponds to the route B_C. The orientation relationship between the grain elongation plane and the subsequent shear plane ($\theta = 71,6^\circ$) that is close to the angle between two $\{111\}$ planes of the fcc Al ($70,5^\circ$) promotes this effective grain refinement for route B_C. All mentioned above makes multi-pass route B_C worthy of investigation.

Many studies have been devoted to understand the material flow [8], deformation behavior [9], and strain distribution [10] during ECAP. Influence of die geometry [11,12], material properties [13], and process parameters [14,15] on strain (in)homogeneity was studied [11,16,17].

Surpassing the known limitations of analytical investigation methods such as slip line field theory and geometric assessments [18,19] or optical analysis [20], finite element analyses (FEAs) have been undertaken in a more realistic approach [8-17,21]. Mainly exposed as results of the influence of friction, die geometry or strain hardening on deformation behavior, FEAs refer mostly at a single pass (the first pass). This is because the first pass involves dramatic changes in microstructure and properties of ECAPed materials and because of the difficulty in preserving the shape and properties of the workpiece for the subsequent passes. But for grain refinement, achieving a high strain through ECAP is essential, so the imposed level of strain involves multi-pass ECAP. The modeling of the whole process especially in 3D space becomes compulsory. The effect of strain path changes in the routes A, B_A, B_C, and C can be revealed only by 3D simulation.

Simulating route A is the simplest, and these are the first results [22-25]. Three methods using different types of dies were used in simulating route A:

A1) The workpiece does not leave the die and the next pass is simulated by reversing the path: the sample is

pressed again through the plastic deformation zone (PDZ) of shear plane, from the horizontal channel back to the vertical channel and so on [20]. The die has 2 channels, and 2 corresponding punches: when pressing with vertical punch, the horizontal punch is out of channel and vice-versa.

A2) The workpiece does not leave the die that has 3 interconnected orthogonal channels in a single plane [23,24]. Till this moment, only 2 passes performed through this method were reported. This type of process is sometime referred to as continuous ECAP.

A3) The workpiece does not leave a rotary die that has 4 orthogonal coplanar channels and one single movable punch [25]. The next pass is simulated by rotating the die until the channel where the sample remained from the previous pass reached the new position right in front of the movable punch.

The simulation of route A has 2 major advantages. First, the working load can be easily monitored because during simulation the longitudinal axis plane does not change its orientation relative to the current extrusion direction. The second advantage is the possibility to use virtual dies with outer and/or inner corner angle of the extrusion channel.

When the route implies rotation of the workpiece around the longitudinal axis (route C, B_A, and B_C) the simulation becomes more complicated. There are two ways for simulating routes C, B_A or B_C: either the workpiece does not leave the die that in turn has n internal PDZs (i.e. shearing zones) with $n + 1$ interconnected (in)coplanar channels [23,26,27] or the billet is firstly twisted around its longitudinal axis and then reinserted into the 3D space of the virtual die [28].

In the first case, the billet must have the length equal to that of the total length of the $n + 1$ channels. The main disadvantage of this method is the huge calculation time because of frequent computational remeshing during solving due to the multiple discontinuity zones. Moreover, the simulation cannot be truly realistic because in practice the vertical channel and the corresponding punch become very long. Therefore, load increases dramatically because of multiple discontinuity zones and friction that increases due to increased dimension in length of the sample. For small dimensions of the cross-section, the buckling of the punch becomes inevitable.

Till now the dies used in simulations were classic dies with two traditional vertical and horizontal channels, respectively. The extruded sample had to be reinserted into the vertical (inlet) channel after a 90° rotation in the virtual space, around its longitudinal axis [28-30]. But it is not clear how these operations were performed, because both of changing in shape of the tetrahedral elements during remeshing and inherent lossing of volume of the virtual workpiece.

The simulation is much simplified in the case of circular cross section of the workpiece [26,27,29] because of full symmetry of the cross section relative to extrusion direction. However, the accurate positioning of the previous deformed workpiece in the inlet die channel remains the sensitive operation together with the inter

object contact formulation between the new contact surfaces.

If simulating route C is quiet similar to the route A when methods A2 and A3 are approachable without compulsory rotation of the workpiece, in simulating routes B_A and B_C the rotation around longitudinal axis becomes indispensable. Continuous ECAP is out of question for a complete B_A and B_C cycle (i.e. 4 passes) because of many difficulties in both simulation and experiments (time calculation, practical implementation, dimension in length of the samples and punch, inherent buckling etc).

To avoid the repositioning of the workpiece for the next pass in performing route B_C, a new approach is proposed in the present study. It consists of using a cubic die with 5 rectangular channels, equal in cross-sectional dimensions, and 5 corresponding punches. At a given moment, three of the channels are blocked and only one punch is moving into the 4th channel to push the workpiece through the 5th empty channel. Relative position of the two channels will define a particular step of the extrusion cycle. Successively ordered combinations of the two channels and corresponding punches develop a complete B_C cycle. The workpiece does not leave the die and no additional repositioning operations are required. To confirm modeling, experimental tests and hardness measurements have been carried out. The simulations results were discussed in terms of accumulated strain using the tracking point method for a chronological monitoring. It was found that route B_C can be conducted in four interconnected operations with better strain homogeneity, without removing the workpiece from the die. The results create opportunities in developing integrated systems designed to perform all ECAP routes for any imposed number of passes.

2. Experimental

2.1. Processing aluminum by multi-pass equal channel angular pressing

In this study, a commercially available 99.5% aluminum alloy (AA 1050) was used. Billets with dimensions of 10 × 10 × 60 mm were annealed at 523 K for 3 h. ECAP was performed at ambient temperature with a speed of 10 mm·s⁻¹, using a die with 5 orthogonal channels and sharp inner angles of $\phi = 90^\circ$ (Fig. 3) and a hydraulic press of 750 kN. The die consists in two half-dies. One of them contains all the 5 channels (4 orthogonal coplanar cross channels and the 5th channel perpendicular on the die's separation plane) and the other one closes the die, as it is suggested in Fig. 3. Each of the 4 coplanar channels has its own active hydraulic piston. The 5th punch is driven by the cylinder of the hydraulic press itself.

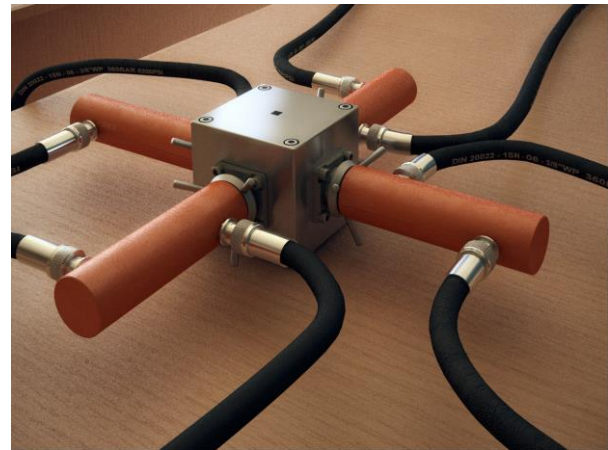


Fig. 3. The die used for multi-pass ECAP

The material was 4 passes ECAPed, route B_C, without removing the sample from the die. As lubricant for samples and die channels zinc stearate was used.

2.2. Simulation of multi-pass equal channel angular pressing

The simulations were carried out using DEFORM 3D software. The stress-strain relationship of the AA 1050 was experimentally obtained by tensile tests carried out according to ISO 6892-1: 2009, using a universal computer-controlled testing machine (Instron 3382). It was found that flow stress vs. strain follows the relation: σ (MPa) = 151.24· $\epsilon^{0.18}$ (Fig. 4) that was nominated in DEFORM 3D as constitutive equation of the material.

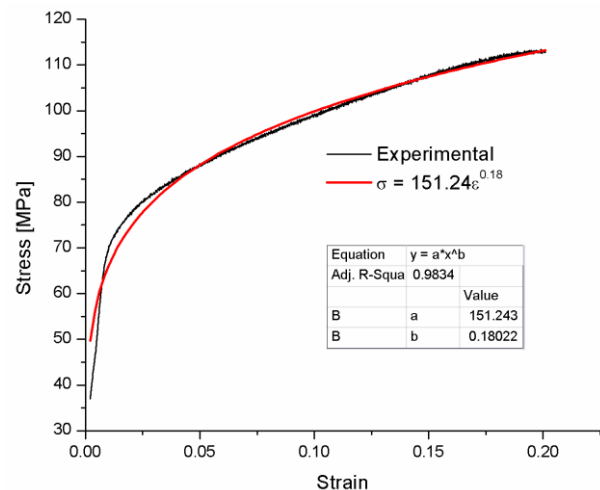


Fig. 4. Plastic flow curve used in simulation

All simulations were carried out at the same temperature and speed conditions as in experimental tests. Simulations took place under a friction coefficient of 0.12. The above value was experimentally determined in a previous study [31], and confirmed in similar works [32].

Because the simulations were carried out at ambient temperature, the hardening behavior was considered independent of strain rate.

In simulating ECAP the mesh that is in contact with the inner walls of the die channels does not distort as the center mesh of the sample. The material can not normally flow when coming in contact with the sharp outer corner, leading in damage of the mesh during extrusion. Because of this, in simulating metal forming, the volume loss is inevitable. There are several causes of volume loss in finite element analysis:

i) if a large time step is used and substepping is disabled, when contact occurs nodes will penetrate slave surfaces, then be repositioned at the end of the step. This repositioning can cause slight volume loss. Over the course of a simulation, this can become significant.

ii) as elements of slave objects stretch around corners of master objects, the elements will cut the corner of the object. The volume that crosses the corner will be lost on remeshing.

To enforce volume constancy of plastic objects, a volume penalty constant must be defined. If the value is too small, unacceptably large volume losses may occur. If the value is too large, the solution may have difficulty converging.

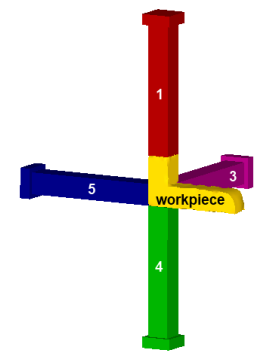
Meshing and re-meshing is the main reason of volume loss in simulating metal forming, which is inevitable. Element volume loss appears in every time-increment step although introducing the incompressibility to penalty function. If reducing the time increment, the volume loss will decrease, but the simulation time will increase. Density of mesh has the same effect as the time increment.

Considering all these, the workpiece was discretized in 12000 tetrahedral elements thus forming a sufficiently fine mesh to reveal localized effects [33]. The volume penalty constant was 10^6 . This value ensures minimum loss of volume during remeshing due to the partial penetration of die by tetrahedral elements, if time increment step of 0.05 s is used.

ECAP cycle was divided into 4 successive operations. To perform successive extrusions via route B_C , the first pass must begin with a punch located in the 4-channels plane. A cycle diagram explains the position and/or the moving of each punch (Table 1). The next pass begins from starting position of the primary (moving) punch that corresponds to the contact with the head of the previous extruded sample. The head of the sample becomes tail and vice-versa. There is no specific time period between two successive passes in simulation.

Table 1. Cycle diagram of multi-pass ECAP simulation

Cycle diagram	Operation #				→	
	1	2	3	4		
Punch #	1	→	×	×	×	Moving punch
	2	⊘	→	×	×	Inside the channel
	3	×	⊘	→	×	
	4	×	×	⊘	→	Outside the channel
	5	×	×	×	⊘	



Before a next operation begins, new inter-object relationship has to be redefined since the primary punch and positions of the other punches are changing according to the cycle diagram.

3. Results and discussions

Ideally, homogenous strain in whole volume of the sample can be obtained if a perfect simple shearing along the bisecting plane of the die channels takes place. Both in practice and simulations, things are different: the deformation is neither a simple shear along a single plane nor homogeneous.

The reason of the heterogeneous behavior of the material passing through PDZ is already known and unanimous accepted [9-11,17,26]. As the material exits from PDZ, strain tends to stabilize and its variation progressively decreases with different ratios. This steady-state deformation behavior could be more visible for longer samples. Obviously, the front and the back regions of the sample are deformed different receiving smaller strain compared to the rest of the sample. That is because of different strain history that in turn is balanced by reversing roles: in the next pass, the tail end becomes head end and vice-versa.

Because of successive changes both of shear plane position and extrusion direction in route B_C analysing final results in terms of accumulated strain makes sense only for a complete 4 passes cycle. For a chronological monitoring of the accumulated strain the tracking point method was used. Three equidistant collinear tracking points ($P_1 \dots P_3$) from top to bottom in the middle longitudinal plane of the sample corresponding to the last operation were nominated. We chose the last step because for the global result this situation is the most relevant. Furthermore, the

validation of the modeling takes into account the confirmation of the accumulated strain by specific measurements in the middle longitudinal plane of the final sample.

Following the path of the three points in the reverse direction (i.e. from the end to beginning), we found their corresponding starting and intermediate positions respectively ($P_1^0 \dots P_3^0, P_1^1 \dots P_3^1, \dots P_1^4 \dots P_3^4$, where the superscript number indicates the pass number). The tracking points and middle longitudinal plane positions are revealed in Fig. 5.

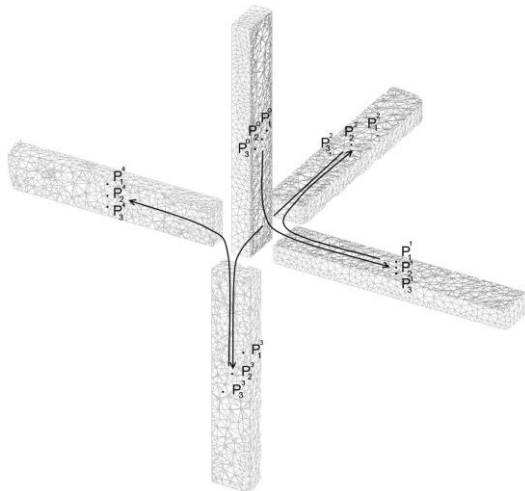


Fig. 5. Schematic path of the tracking points from the middle longitudinal plane suggesting differences in displacement and their corresponding positions during multi-pass ECAP operations (route B_C)

As one can see, due to the successive changing of the extrusion direction and shearing plane, the three points are not all in step with each other when they are passing through PDZ. But the defined tracking points keep their coplanarity remaining quasi-collinear. Fig. 6 shows the current strain distribution of the corresponding longitudinal planes and the accumulated strain vs. extrusion time for the three tracking points. Because the extruding directions were changed successively the category axis name was designated as extrusion time instead of punch stroke.

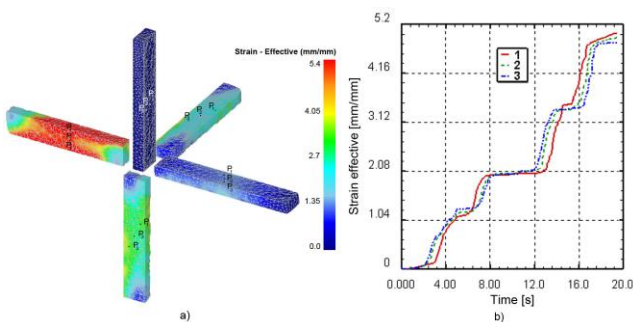


Fig. 6. The simulated strain distribution for the tracking points: a) current strain distribution in the corresponding longitudinal planes; b) accumulated strain during multi-pass ECAP

Naturally, the strain increases continuously throughout the multi-pass extrusion. As expected, there is a difference in strain between the tracking points according to their positioning for the given step, especially for the second and the third pass when inherent difference of displacement appears. Starting with the second pass, the differences in strain become visible and the extreme points P_1 and P_3 receive different strain. During the third pass, the roles are changing: the point that is passing through PDZ near to the inner corner of the extrusion channels receives greater strain. In the last pass, the strain distribution is balanced, strain corresponding to P_1 and P_3 respectively tends to equalize. The level of the accumulated strain is in good agreement with the theory.

There are several methods to validate the model in simulation of deformation processes. Fitting the predicted and experimental working-load is one of them [32], but it does not reveal the final result. The final strain distribution is a major milestone of the multi-pass ECAP study, confirming the accumulated strain history. Fitting the experimental and simulated strain is the most appropriate way to validate the simulation [35]. Therefore, the billet was processed until it arrived at the middle of the last pass. The sample removed by disassembling the die was then longitudinally sectioned by electro-discharging to get a proper surface for the microhardness test [36]. After determining from simulation the trajectories of $P_1 \dots P_3$, the corresponding lines were drawn on the prepared surface of the sample (Fig. 7).

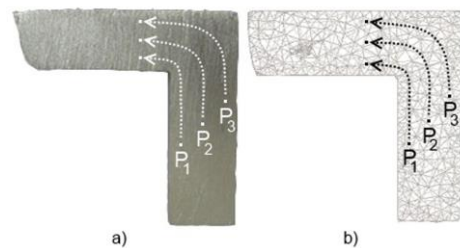


Fig. 7. Schematic path for microhardness measurements (longitudinal section) a) experimental, b) simulation

Fig. 8 shows the simulated effective strain (accumulated) corresponding to the last pass vs. time (a) and the microhardness for the tracking points $P_1 \dots P_3$ (b) following the schematic path suggested in Fig. 7. As one can see the simulation and the experiment fit in qualitative terms.

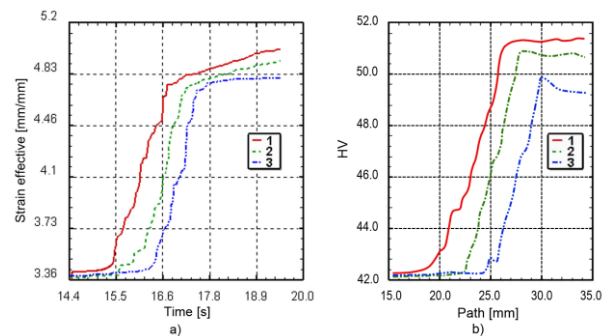


Fig. 8. The simulated distribution of the accumulated strain for (a) the last pass and (b) the experimentally determined microhardness along identical routes of the tracking points

4. Conclusions

Because traditional ECAP is a discontinuous process, for industrial implementation, processing materials by ECAP through successive extrusions in a continuous manner became necessary. In this work it is shown that the inherent loss of volume by removing the distorted head and tail of the samples processed by traditional ECAP can be avoided by multi-pass ECAP. Furthermore, a complete processing cycle consisting in 4 passes via route B_C balances the wellknown nonuniformity of the strain during ECAP. Experimental ECAP using a special die having 5 orthogonal channels and corresponding hydraulic pistons was performed successfully. To confirm the feasibility of the purposed solution, a 3D FEA was performed to simulate the behavior and the accumulated strain distribution of aluminum during multi-pass ECAP without removing the workpiece from the die. Experimental tests and hardness measurements along the dedicated tracking point routes were performed in order to test the simulation. It was found that the hardness and the accumulated strain fit in qualitative terms, confirming the strain history and validating the modeling.

The results provide a useful analysis tool in developing integrated systems designed to perform different ECAP routes that facilitates the deployment of ECAP in industry.

References

- [1] P. Yang, K.-H. Yang, *Adv. Mater. Res.* **629**, 198 (2013).
- [2] D. Raducanu, V. D. Cojocaru, I. Cinca, I. Ichim, A. Sichin, *J. Optoelectron. Adv. Mater.* **9**(11), 3346 (2007).
- [3] V. Chertes, R. L. Orban, I. Vida-Simiti, D. Salomie, J. Optoelectron. Adv. Mater. **14**(5-6), 551 (2012).
- [4] S. Surendarnath, K. Sankaranarayanan, B. Ravisankar, *Mater. Manuf. Process.* **29**(6), 691 (2014).
- [5] V. M. Segal, I. J. Beyerlein, C. N. Tome, V. N. Chuvildeev, V. I. Kopylov, Nova Science Publishers, New York (2010).
- [6] Y. Iwahashi, M. Furukawa, Z. Horita, M. Nemoto, T. G. Langdon, *Metall. Mater. Trans.* **29**(9), 2245 (1998).
- [7] Y. T. Zhu, T. C. Lowe, *Mater. Sci. Eng. A* **291**, 46 (2000).
- [8] J. H. Li, Z. J. Yu, D. Z. Xiao, *App. Mec. Mater.* **423-426**, 267 (2013).
- [9] K. V. Ivanov, E. V. Naydenkin, *Mater. Sci. Eng. A*, **606**, 313 (2014).
- [10] T. Suo, Y. Li, Y. Guo, Y. Liu, *Mater. Sci. Eng. A*, **432**, 269 (2006).
- [11] V. Patil Basavaraj, U. Chakkingal, T. S. Prasanna Kumar, *J. Manuf. Process.* **17**, 88 (2015).
- [12] A. V. Perig, I. G. Zhibankov, V. A. Palamarchuk, *Mater. Manuf. Process.* **28**(8), 910 (2013).
- [13] M. Ebrahimi, F. Djavanroodi, C. Gode, K. M. Nikbin, *Revue de Met. Cahiers d'Informations Tech*, **110**(5), 341 (2013).
- [14] F. Djavanroodi, M. Ebrahimi, *Mater. Sci. Eng. A* **527**, 1230 (2010).
- [15] S. C. Yoon, H.-G. Jong, S. Lee, H. S. Kim, *Comput. Mater. Sci.* **77**, 202 (2013).
- [16] D. Salcedo, C. Luis, I. Puertas, *Mater. Manuf. Process.* **29**(4), 434 (2014).
- [17] C. J. Luis Pérez, R. Luri, *Mater. Manuf. Process.* **26**(9), 1147 (2011).
- [18] C. O. Rusănescu, M. Rusănescu, T. Iordănescu, F. V. Anghelina, *J. Optoelectron. Adv. M.* **15** (7-8), 718 (2013).
- [19] I. N. Popescu, V. Bratu, M. Rosso, C. Popescu, E. V. Stoian, *J. Optoelectron. Adv. Mater.* **15** (7-8), 712 (2013).
- [20] L. Ciobanu, C. Dumitras, *J. Optoelectron. Adv. Mater.* **13** (2), 130 (2011).
- [21] A. M. Vitalariu, R.I. Comaneci, C. Dumitras, *J. Optoelectron. Adv. Mater.* **9** (11), 3419 (2007).
- [22] M. W. Fu, M. S. Yong, Q. Pei, H. H. Hng, *Mater. Manuf. Process.* **2**(5), 507 (2006).
- [23] H. S. Kim, *Mater. Sci. Eng. A* **328**, 317 (2002).
- [24] Y.-L. Yang, S. Lee, *J. Mater. Process. Technol.* **140**, 583 (2003).
- [25] Y. C. Yuan, A. B. Ma, J. H. Jiang, D. H. Yang, *J. Mater. Eng. Perform.* **20**(8), 1378 (2011).
- [26] W. J. Kim, J. C. Namgung, J. K. Kim, *Scripta Mater.* **53**, 293 (2005).
- [27] E. Cerri, P. P. de Marco, P. Leo, *J. Mater. Process. Technol.* **209**, 1550 (2009).
- [28] Y. G. Jin, I.-H. Son, S.-H. Kang, Y.-T. Ima, *Mater. Sci. Eng. A* **503**, 152 (2009).
- [29] S. Xu, G. Zhao, Y. Luan, Y. Guan, *J. Mater. Process. Technol.* **176**, 251 (2006).
- [30] Y. W. Tham, M. W. Fu, H. H. Hng, M. S. Yong, K. B. Lim, *J. Mater. Process. Technol.* **192-193**, 121 (2007).
- [31] C. Chirita, R. Comaneci, L. Zaharia, A.C. Hanganu, *Annals of DAAAM for 2007 & Proc. 18th Intern. DAAAM Symp.*, Ed. B. Katalinic, Zadar, Croatia, DAAAM International, Vienna, 2007, p. 139.
- [32] R. B. Figueiredo, P. R. Cetlin, T. G. Langdon, *Mater. Sci. Eng. A* **518**, 124 (2009).
- [33] R. B. Figueiredo, P. R. Cetlin, T. G. Langdon, *Acta Mater.* **55**, 4769 (2007).
- [34] H. Hongjun, Z. Zhiye, L. YunYang, *Mater. Res.* **17**(4), 1056 (2014).
- [35] A. A. Smolyakov, V. P. Solovyev, A. I. Korshunov, N. A. Enikeev, *Mater. Sci. Eng. A* **493**, 148 (2008).
- [36] A. P. Zhilyaev, T. G. Langdon *Mater. Res.* **16**(3), 586 (2013).